

Transition Measurement on the Natural Laminar Flow wing of the Non-Powered Experimental Airplane for Supersonic Transport

Hiroki Sugiura*, Kenji Yoshida*, Naoko Tokugawa*, Shohei Takagi*, Akira Nishizawa*
*National Aerospace Laboratory, Chofu, Tokyo 182-8522, JAPAN

Transition measurement on the natural laminar flow wing of Non-powered Experimental Airplane for Supersonic Transport was conducted at Mach 2.0 and 1.2. Increase of perturbation in amplitude of output signals for hot-films placed along the wing chord indicates transition from laminar to turbulent boundary layer. Results by hot-film and Preston tubes proved that transition point is located downstream of the half chord of the wing.

Keywords: *transition measurement, compressible boundary layer, supersonic transport*

1. Introduction

NAL is currently developing an unmanned non-powered supersonic experimental plane called "NAL's Experimental Airplane for Supersonic Transport (NEXST-1)". In the design of NEXST-1, following design concepts are applied to reduce drag of supersonic transport around Mach 2.: a) arrow wing planform, b) warped wing, c) Area-ruled body, and d) supersonic natural laminar flow wing concept. The last concept is effective for reducing the friction drags of the wing that occupies nearly half of the total drag of supersonic transport. NEXST-1 is the first original attempt to apply this concept to the configuration of supersonic transport.

This concept is based on an optimum pressure distribution to achieve the delay of transition (Ref.1). The amplification of disturbance by cross-flow instability dominates in the boundary layer transition on highly swept wings. In order to suppress the transition due to cross-flow instability, the pressure falls very rapidly in the leading edge region of the supersonic natural laminar flow wing, so as to minimize the cross-flow velocity components and this leads to suppress the transition due to cross-flow instability. Afterward the leading edge region, gradually favorable pressure gradient suppress the Tollmien-Schlichting instability (Ref.2). As for the transition due to the attachment line contamination, the leading edge radius of the wing is small and the Reynolds number based on the edge velocity parallel to the leading edge is well below Poll's criterion (Ref.3).

The experimental validation of the concept, however, is not been conducted yet because there are few large supersonic wind tunnels with very low turbulence level. In the present research, transition measurements in an indraft supersonic wind tunnel and in continuous tunnels were conducted at Mach 2 and at Mach 1.2 to validate the concept before the flight tests.

2. M=2 Results in the Indraft Wind Tunnel

2.1 Testing Facility

The transition measurement was conducted in the 61cm indraft supersonic wind tunnel of Fuji Heavy Industries in Japan. Indraft tunnel has lower turbulence level than general blowdown tunnel. Turbulence level was measured by total pressure tube installed in AEDC 10 degree cone model in the present experiment. Fluctuating pressure coefficient was 0.05%, which is about less than one tenth of the value of general supersonic tunnel.

2.2 Models

Two 15.7% scale half wing models of NEXST-1 (Fig.1) was used in the tests. One of them is for pressure measurement and the other is for transition measurement. Both of them has same configuration.

The pressure model has 15 static pressure orifice at $y/s=0.3$ chord, 14 at $y/s=0.5$ chord, and 11 at $y/s=0.7$ chord.

The transition model has multi-element hot-film sensors at $y/s=0.3$ chord and $y/s=0.7$ chord.

Reynolds number based on the mean aerodynamic chord of the present model is 4.7 million at Mach 2.

2.3 Pressure Measurement Result

Designed pressure distribution was realized at the angle of attack of 2.7 degrees on the model (Fig.2). The present result and the computational result agree fairly well (Fig.2). The Difference of both results in the value of angle of attack is due to half model testing. Downwash distribution towards the wing changes in general half model testing due to the existence of tunnel wall boundary layer and splitter plates and the angle of attack.

2.4 Transition Measurement Result

The intensities of shear-stress fluctuation along the wing chord is shown in Fig.3. The amplitude of the fluctuation stays at small level in the laminar region and grow rapidly in the transition region. It shows a peak in the transition region and stays constant at relatively small level in the turbulent region.

At design angle of attack ($\alpha=2.7$ degree), location of the end of transition is downstream of 55% chord length (Estimated location is $x/c=0.65$). At 1.5 degree, location of the onset of transition is even downstream than that at the design angle of attack. This shows that the natural laminar flow is sustained over relatively large range of angles of attack. At $\alpha=-1$ degree, the wing has gradually favorable pressure distribution similar to the conventional supersonic and the end of transition moves forward to $x/c=0.35$.

3. M=2 Results in the Continuous Wind Tunnel

Transition measurement in the ONERA S2MA continuous supersonic tunnel will be also conducted this October. The continuous tunnel achieve higher Reynolds number than the indraft tunnel and the effect of Reynolds number and free stream disturbance on the transition location of the natural laminar flow wing will be studied.

4. M=1.2 Experiments and Results

4.1 The Testing Facility and the Model

In order to verify the natural laminar flow wing design concept at off-design Mach number, transition measurement was conducted at Mach 1.2.

The transition measurement was conducted in NAL 2m transonic wind tunnel. It is a continuous, closed-circuit wind tunnel. Reynolds number based on the mean aerodynamic chord of the present model at Mach 1.2 is 5.4 million when total pressure is 60kPa.

23.3% scale full wing-body model (Fig.4) was used in the tests. It has 11 static pressure orifice at $y/s=0.3$ chord, 10 at $y/s=0.5$ chord, 10 at $y/s=0.7$ chord, and 10 orifice on the left side of the fuselage. The model has multi-element hot-film sensors at $y/s=0.3$ chord and $y/s=0.7$ chord.

4.2 Pressure Measurement Result

The designed pressure distribution was realized at the angle of attack of 0.5 degree at $y/s=0.3$. At $y/s=0.7$, the designed distribution was realized at the angle of attack of 0 degree. The following transition measurement was conducted at those angles of attack.

4.3 Transition Measurement Results

Fig.5 and 6 shows the intensities of shear-stress fluctuation along the wing chord.

Fig.5 and 6 shows that when the total pressure is 60kPa, laminar boundary layer was achieved up to 52% chord at $y/s=0.7$ (at 0.5 degree of angle of attack) and up to 41% chord at $y/s=0.3$ (at 0 degree of angle of attack) (There are no hot-film sensor downstream of this location.).

Fig.7 shows the location of the onset and the end of transition measured by Preston tubes. Fig.7 shows that when the total pressure is 60kPa, laminar boundary layer was achieved up to 40% chord at $y/s=0.7$ and up to 50% chord at $y/s=0.3$ (There are no hot-film sensor downstream of this location.) . This agrees well with the results by hot-film sensors.

5. Concluding remarks

- 1) Transition location on the natural laminar flow wing of the supersonic experimental airplane were measured using hot-film sensors and Preston tubes at M=2 and at M=1.2.
- 2) The end of the transition moved far downstream by applying the supersonic natural laminar flow wing concept at Mach 2.

References

- 1) Yoshida, K. -Overview of NAL 's Program including the Aerodynamic Design of the scaled Supersonic Experimental Airplane, VKI Special Course of "Fluid Dynamics Research on Supersonic Aircraft", RTO-EN-4, No.15,1998.
- 2) Arnal, D. -Boundary Layer Transition: Prediction, Application to Drag Reduction, "Special course on Progress in Transition Modeling", AGARD Report 793,1993.
- 3) Poll, D.I.A. -Transition in the infinite swept attachment line boundary layer, Aeronaut. Q.,vol.30, pp.607-,1997.



Figure 1. 15.7% scale half wing model of NEXST-1.

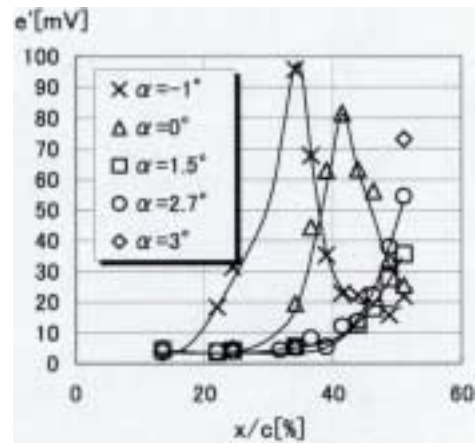


Figure 3. The intensities of shear-stress fluctuation at $y/s=0.7$ on the natural laminar flow wing of the NEXST-1 at Mach 2.

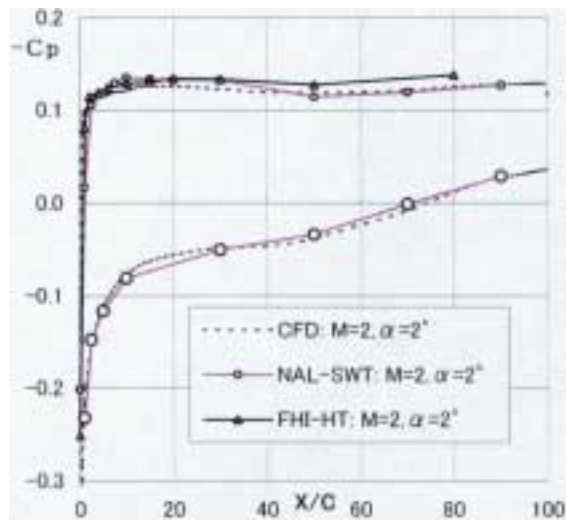


Figure 2. Pressure distributions at $y/s=0.7$ on the natural laminar flow wing of the NEXST-1 at Mach 2.



Figure 4. 23.3% scale full wing-body model of NEXST-1.

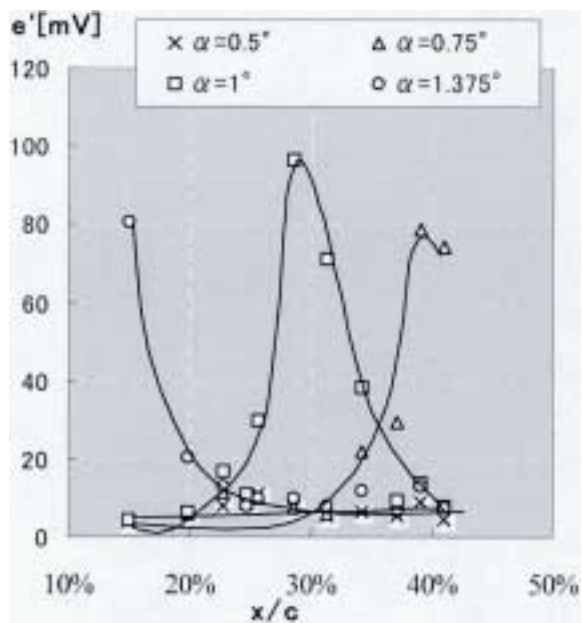


Figure 5. The intensities of shear-stress fluctuation at $y/s=0.3$ on the natural laminar flow wing of the NEXST-1 at Mach 1.2 60kPa.

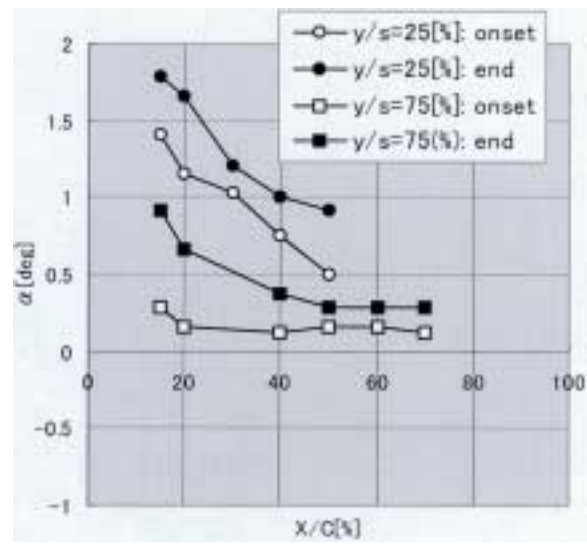


Figure 7. The location of the onset and the end of transition measured by Preston tubes

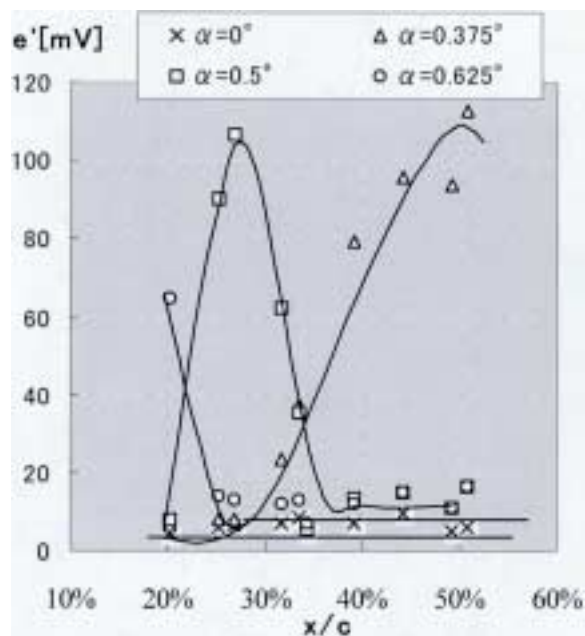


Figure 6. The intensities of shear-stress fluctuation at $y/s=0.7$ on the natural laminar flow wing of the NEXST-1 at Mach 1.2 60kPa.